Drug Resistance

Deutsche Ausgabe: DOI: 10.1002/ange.201510079
Internationale Ausgabe: DOI: 10.1002/anie.201510079

Antarlides: A New Type of Androgen Receptor (AR) Antagonist that Overcomes Resistance to AR-Targeted Therapy

Shun Saito, Takahiro Fujimaki, Watanalai Panbangred, Yasuhiro Igarashi, and Masaya Imoto**

Abstract: *Prostate cancer is treated with androgen receptor (AR) antagonists but most patients experience disease progression after long-term treatment with these compounds. Therefore, new AR antagonists are required for patient follow-up treatment. In the course of screening for a new AR antagonist, we isolated the novel compounds antarlides A–E (**1**–**5**) from Streptomyces sp. BB47. Antarlides are mutually isomeric with respect to the double bond and have a 22-membered-ring macrocyclic structure. The full stereostructure of **1** was established by chemical modifications, including methanolysis, the Trost method, acetonide formation, and the PGME method. **1**–**5** inhibited the binding of androgen to ARs in vitro. In addition, **2** inhibited the transcriptional activity of not only wild-type AR but also mutant ARs, which are seen in patients with acquired resistance to clinically used AR antagonists. Therefore, antarlides are a potent new generation of AR antagonists that overcome resistance.*

Prostate cancer is one of the most commonly diagnosed cancers among men worldwide.[1] Androgen receptor (AR) signaling plays a central role in the malignancy of prostate cancers,[2] and androgen deprivation by medical or surgical castration is the standard first-line treatment for men with advanced prostate cancer. Over time, most men will progress to a more aggressive form of the disease called castration-resistant prostate cancer (CRPC). CRPC is commonly associated with sustained activity of AR signaling through AR gene overexpression/amplification.[3] The continued reliance on AR signaling in CRPC has led to the development of AR antagonists that compete with androgens, such as testosterone and dihydrotestosterone (DHT), for binding to the AR. First-generation AR antagonists, such as flutamide and bicalutamide, have a low affinity for the AR and, as a result, insufficiently block AR signaling.[4] Moreover, long-term treatment with these AR antagonists can lead to AR point mutations which are linked to the development of resistance.[5] A second-generation AR antagonist, enzalutamide, has evolved from the need for more effective and long-term AR inhibition and has been recently approved by the U.S. Food and Drug Administration.[6] However, despite the initial response to enzalutamide, resistance also develops in most patients with metastatic CRPC. These observations, combined with the limited impact of existing AR antagonists, motivated us to develop novel AR antagonists. We therefore screened microbial extracts to find new AR antagonists that could inhibit the binding of [^{3}H]-labeled DHT to the AR in an in vitro binding assay.[7] From this screen, we isolated five novel compounds named antarlides A–E (**1**–**5**) from the fermentation extract of *Streptomyces* sp. BB47.[8] In this Communication, the isolation, structure elucidation, and biological activities of **1**–**5** are reported.

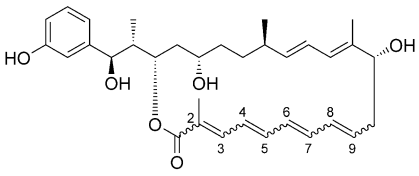

Antarlides A–E (**1**–**5**)

1: $\Delta^{2,3} = E$, $\Delta^{4,5} = E$, $\Delta^{6,7} = E$, $\Delta^{8,9} = E$.
2: $\Delta^{2,3} = E$, $\Delta^{4,5} = Z$, $\Delta^{6,7} = E$, $\Delta^{8,9} = Z$.
3: $\Delta^{2,3} = E$, $\Delta^{4,5} = E$, $\Delta^{6,7} = Z$, $\Delta^{8,9} = Z$.
4: $\Delta^{2,3} = E$, $\Delta^{4,5} = E$, $\Delta^{6,7} = Z$, $\Delta^{8,9} = E$.
5: $\Delta^{2,3} = E$, $\Delta^{4,5} = Z$, $\Delta^{6,7} = E$, $\Delta^{8,9} = E$.

Streptomyces sp. BB47 was cultured in A3MP producing medium at 30 °C for 6 days, and the whole culture broth was extracted with EtOAc. This extract was partitioned between 10 % aqueous MeOH and *n*-hexane, and the aqueous MeOH layer was further separated between EtOAc and H_2O (pH 10). The EtOAc-soluble fraction was fractionated by centrifugal liquid–liquid partition chromatography and reverse-phase column chromatography, followed by HPLC purification on a C30 column, to yield antarlides A–E (**1**–**5**). All isolation steps were carried out in the dark because antarlides are unstable under ambient light.

Antarlide A (**1**) was obtained as a pale yellow powder and the molecular formula was found to be $C_{33}H_{44}O_6$ by high-resolution ESITOF mass spectrometry ($[M-H]^-$ $m/z =$ 535.3055). The IR spectrum of **1** displayed absorption bands at 3362 and 1670 cm^{-1}, indicating the presence of hydroxy and carbonyl groups. The UV/Vis absorption bands at $\lambda = 337$ nm suggested the presence of a polyene moiety. ^{1}H and ^{13}C NMR data, in combination with the HSQC analysis, revealed the presence of 33 carbons attributable to one carbonyl, eighteen sp^2 carbon atoms (fourteen are proton-bearing, one is oxy-

[*] S. Saito, Dr. T. Fujimaki, Prof. M. Imoto
Bioscience and Informatics, Keio University
3-14-1 Hiyoshi, Kohoku-ku, Yokohama, 223-8522 (Japan)
E-mail: imoto@bio.keio.ac.jp
Prof. W. Panbangred
Biotechnology, Mahidol University
Bangkok 10400 (Thailand)
Prof. Y. Igarashi
Biotechnology Research Center, Toyama Prefectural University
5180 Kurokawa, Imizu, Toyama 939-0398 (Japan)
E-mail: yas@pu-toyama.ac.jp

Supporting information for this article is available on the WWW under http://dx.doi.org/10.1002/anie.201510079.

genated), four sp^3 methylene moieties, six sp^3 methine centers (four are oxygenated), and four methyl groups. One carbonyl and eighteen sp^2 carbon atoms require the presence of two rings from the unsaturation degrees of the formula of **1**.

The full planar structure of **1** was assigned through interpretation of 1D and 2D NMR spectroscopic data recorded in [D_6]acetone (see Table S1 in the Supporting Information). A detailed analysis of the ^1H–^1H COSY spectrum revealed five partial proton–proton connectivities (see Figure 1 for atom labelling): a) from H3 to H11, b) from H13 to H15, c) from H16 to H21 and methyl group proton H16a, d) from H22 to H23 and methyl group proton H22a, and e) from H27 to H29.

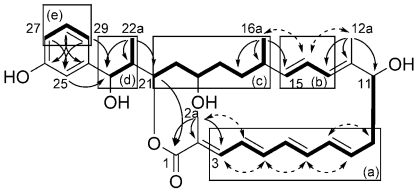

Figure 1. Planar structure of **1** determined by 2D NMR analysis. Bold lines indicate COSY-determined correlations; arrows indicate selected HMBC correlations; dashed arrows show selected NOESY correlations.

Interpretation of the HMBC NMR data allowed the ^1H–^1H COSY-defined fragments of **1** to be connected, as shown in Figure 1. The linkage of the partial structures between (a) and (c) was established by HMBC correlations from proton H2a to carbons C1, C2, and C3, and from H21 to C1. Furthermore, the partial structure (c) and the correlations from proton H12a to carbons C11, C12, and C13 and from H16a to C15, C16, and C17 carbon centers constructed a macrocyclic structure of a 22-membered ring. This macrocyclic ring was connected to the partial structure (d) on the basis of HMBC correlations from H22a to C21. The remaining partial structure (e) was connected to a three-carbon unit (C24, C25, C26) on the basis of HMBC correlations from H28 to C24 and C26, from H27 to C25, and from H29 to C25. These data established a benzene ring possessing an oxygen-bearing C26 carbon atom ($\delta = 157.2$ ppm). This benzene ring was expanded to the partial structure (d) based on HMBC correlations from H25 to C23 and from H29 to C23. The molecular formula of **1** indicated four protons left to be assigned but these protons could be assigned to the hydroxy protons at C11 ($\delta = 77.2$ ppm), C19 (68.8 ppm), C23 (75.5 ppm), and C26 centers (157.2 ppm).

The double bond geometries of **1** were assigned by analysis of NOESY correlations as shown in Figure 1. C2−C3, C4−C5, C6−C7, C8−C9, C12−C13, and C14−C15 double bonds were assigned as *E*, *E*, *E*, *E*, *E*, and *E* on the basis of NOESY correlations for H2a−H4, H3−H5, H5−H7, H7−H9, H8−H10, H12a−H14, and H14−H16a.

The instability of antarlides is likely due to the ring strain of the all-*trans* polyolefinic macrocyclic structure. To release the strain to avoid the double-bond isomerization, the lactone linkage of **1** was cleaved by methanolysis with NaOMe in MeOH to yield the methyl ester **6** (Scheme 1).[9]

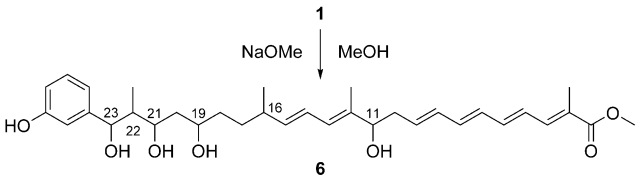

Scheme 1. Methanolysis of **1** to yield ester **6**.

The stereochemistry at the C11 and C19 carbon centers of **6** were determined by application of the Trost ester NMR method.[10] Treatment of **6** with (*R*)-methoxyphenylacetic acid (*R*-MPA) and (*S*)-methoxyphenylacetic acid (*S*-MPA), yielded the (*R*)-Trost ester **7a** and (*S*)-Trost ester **7b**, respectively. Analysis of the chemical shift differences ($\Delta\delta_{R-S}$) between **7a** and **7b** revealed that the C11 and C19 positions have *R* and *S* absolute configurations (Figure 2). The configuration of the C21 and C23 positions in **6** could not be assigned.

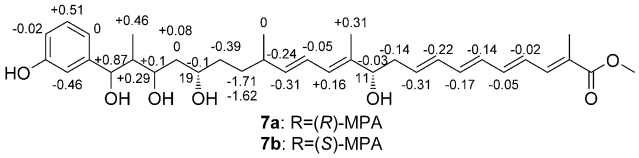

Figure 2. $\Delta\delta_{R-S}$ values for the Trost esters **7a**/**7b** of **6**.

Treatment of **6** with 2,2-dimethoxypropane and pyridinium *p*-toluenesulfonate (PPTS) in acetone yielded the monoacetone ketal **8**, resulting from ketal formation at the C19 and C21 hydroxy groups (Figure 3). ^{13}C NMR chemical shifts of the acetonide methyl groups were detected at $\delta =$ 19.2 and 29.8 ppm (HSQC spectral data), indicating that the six-membered 1,3-dioxane ring was in a chair conformation.[11] The configuration of the hydroxy groups at the C19 and C21 carbon atoms was therefore assigned as *syn* and thus the C21 atom has an *S* absolute configuration.

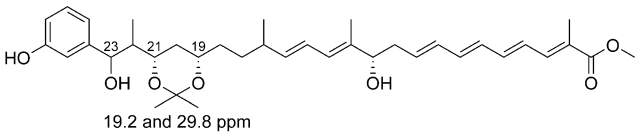

Figure 3. The chemical structure of acetonide **8** showing the ^{13}C NMR chemical shifts of acetonide methyl carbon atoms.

Although the absolute configurations at the C22 and C23 positions of **1** were not assignable, the relative configuration from C21 to C23 of **1** could be determined by NOESY and *J*-based configuration analysis. To elucidate the relative configuration of **1** by the *J*-based NMR method, $^3J_{H,H}$ and $^2J_{C,H}$ values were obtained from ^1H NMR and *J*-resolved HMBC spectra. As for the C21–C22 axis, the small coupling constants $^3J_{H21,H22} = 4.5$ Hz and $^2J_{C21,H22} = 2.2$ Hz inferred a *gauche* relationship for the oxygen substituent at C21 and

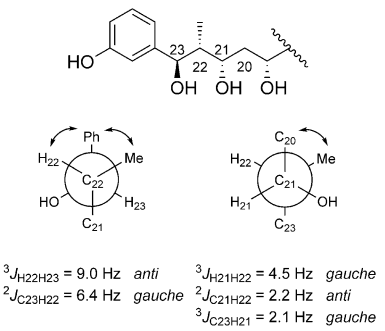

Figure 4. ^{1}H–^{1}H, ^{13}C–^{1}H coupling constants and relative configuration determined for C21–C23. Arrows show NOESY correlations.

the C22a methyl group (Figure 4). Therefore, an *R* absolute configuration for the C22 center was established. Additionally, the large coupling constants $^3J_{H22,H23} = 9.0$ Hz and $^2J_{C23,H22} = 6.4$ Hz inferred an *anti* relationship for the C22a methyl and C23-OH groups with respect to the C22–C23 axis. The C23 center was thus determined to have an *R* absolute configuration.

To determine the absolute configuration of the remaining C16 methyl center, compound **9**, a peracetylated derivative of **6**, was subjected to oxidative cleavage employing $RuCl_3$ as a catalyst to provide carboxylic acid **10**.[12] Compound **10** was then converted into mono-(*R*)- and (*S*)-PGME amides (**11a** and **11b**, respectively).[13] Analysis of chemical-shift differences ($\Delta\delta_{S-R}$) between **11a** and **11b** revealed that the C16 center has an *R* absolute configuration (Scheme 2).

It is known that the *cis–trans* geometric isomerism in a polyene system is affected by light or heat. When methanol solutions of **2**–**5** were exposed to room light in a capped clear

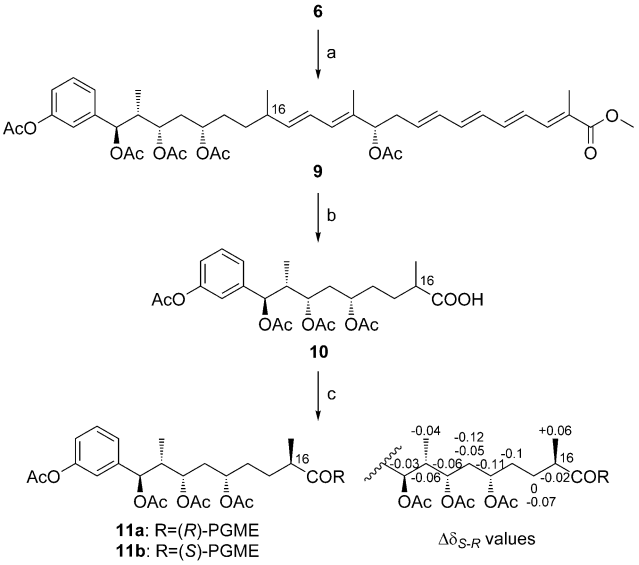

Scheme 2. Preparation of compounds **11a/11b**. Reagents and conditions: a) acetic anhydride, pyridine, room temperature; b) $NaIO_4$, $RuCl_3$, $MeCN/CCl_4/H_2O$, 0 °C; c) (*R*,*S*)-PGME, PyBOP, HOBt, triethylamine, dry DMF, room temperature. PyBOP = (1H-benzotriazol-1-yloxy)tris(pyrrolidino)phosphonium hexafluorophosphate; HOBt = 1-hydroxybenzotriazole.

Eppendorf vial, these compounds isomerized to **1** within 2 hours (Figure S72). Based on this observation, as well as on the fact that **1** is the main product in the culture, it is conceivable that the strain produces **1** as a "natural product", which then isomerizes to other congeners during bacterial cultivation and/or compound isolation. The asymmetric centers in **2**–**5** are most likely to have the same absolute configurations as those in **1**.

Antarlides were tested for their AR-DHT binding inhibition activities in vitro.[14] The compounds inhibited the binding of DHT to ARs in a dose-dependent manner. Their IC_{50} values were circa 16 μM (Table 1). Furthermore, these inhibitory activities were equal to that of hydroxyflutamide ($IC_{50} = 17.7$ μM), which is clinically used for the treatment of prostatic diseases. On the other hand, antarlides did not show inhibitory activity against the binding of estradiol to estrogen receptors (ER) at concentrations up to 100 μM (Table 1). These data suggested that antarlides specifically block the binding of androgen to the ligand-binding domain of AR in vitro.

Table 1: IC_{50} values (μM) for the inhibition of binding of DHT to the AR or estradiol to the ER by antarlides **1**–**5**.

Compound	**1**	**2**	**3**	**4**	**5**	Hydroxy flutamide
AR	20.0	14.7	13.8	13.6	17.9	17.7
ER	>100	>100	>100	>100	>100	>100

Among the congeners, antarlide B (**2**) is more stable, therefore, AR antagonist activities against prostate cancer cells were evaluated by using **2**. Prostate-specific antigen (PSA) is a 33 kDa serine protease, whose expression is triggered by androgen-mediated action of the AR. As shown in Figure 5, **2** inhibited DHT-induced expression of endogenous PSA mRNA in LNCaP cells (androgen-sensitive human prostrate adenocarcinoma cells) with an IC_{50} value of 0.18 μM. Furthermore, **2** was found to inhibit DHT-induced cell growth in LNCaP cells with an IC_{50} value of 0.31 μM. These AR antagonist activities of **2** were superior to the respective activities of hydroxyflutamide (IC_{50} values 1.3 and 1.2 μM, respectively).

Emergence of a mutant AR has been shown to be linked to resistance to first- and second-generation AR antagonists (T877A for flutamide resistance,[15] W741C for bicalutamide resistance,[16] and F876L for enzalutamide resistance[17]). Therefore, we next evaluated whether antarlides are capable of inhibiting the activity of these mutant ARs. As shown in Figure 6, antarlide B (**2**) inhibited DHT-induced transcriptional activity not only of the wild-type AR but also of all mutant ARs that we tested, indicating that antarlides could overcome resistance to AR antagonists.

Furthermore, the F876L mutation of AR has been reported to confer an antagonist-to-agonist switch specific for enzalutamide.[17] Indeed, as shown in Figure 7, the F876L AR mutant was predominantly cytoplasmic, and treatment of cells with enzalutamide induced nuclear translocation of the mutant AR, indicating that enzalutamide acts as an agonist in

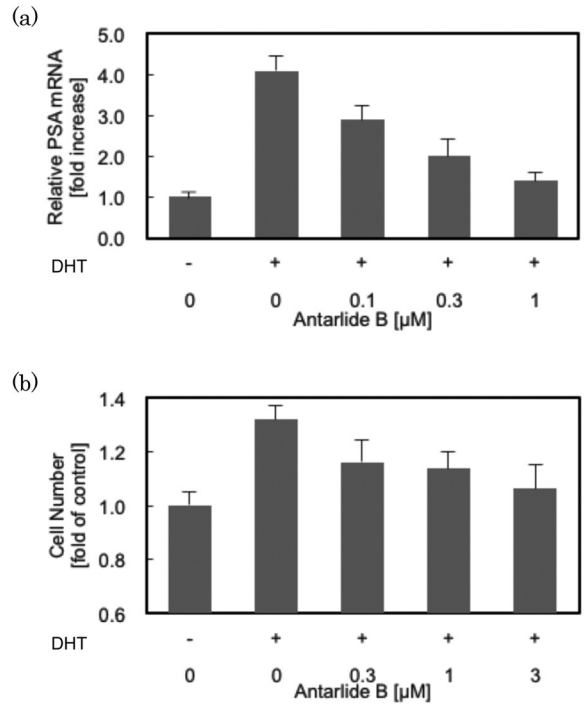

Figure 5. Effect of antarlide B (**2**) on DHT-induced a) expression of endogenous PSA mRNA and b) cell growth.

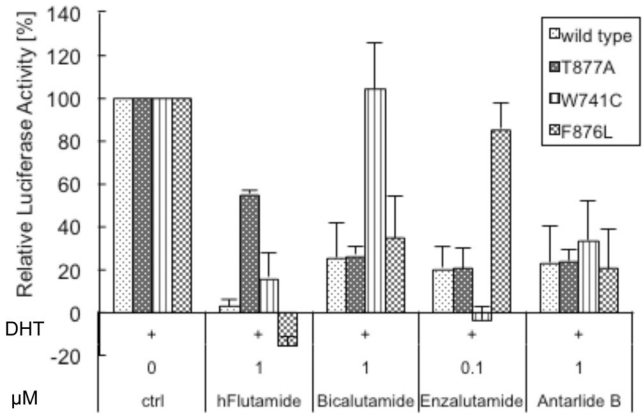

Figure 6. Effect of **2** on transcriptional activity of wild-type or mutant AR (hFlutamide = hydroxyflutamide).

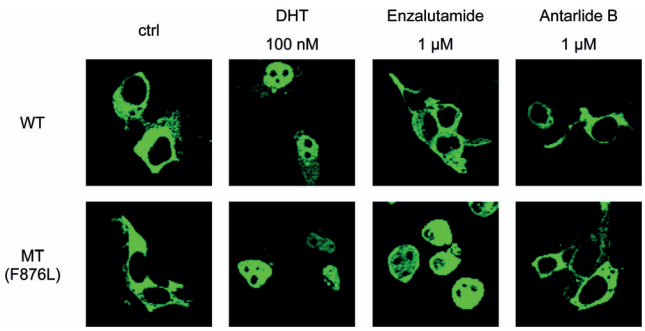

Figure 7. Effect of antarlide B (**2**) on nuclear translocation of wild-type and mutant AR.

F876L mutant AR-expressing cells. On the other hand, **2** did not induce nuclear translocation of the F876L mutant AR. These results indicated that **2** does not act as an agonist in enzalutamide-resistant cells.

In conclusion, we have discovered the novel compounds antarlides A–E (**1**–**5**), isolated from *Streptomyces* sp. BB47, which act as AR antagonists. Antarlides are structurally distinct from all known AR antagonists. Antarlide B (**2**) bound AR specifically, and showed AR antagonistic activity towards prostate cancer cells. In addition, **2** inhibited the transcriptional activity of wild-type and mutant AR, which are seen in patients with acquired resistance to current clinically used AR antagonists. Therefore, antarlides may have the potential to provide the basis for third-generation AR antagonists that overcome resistance to existing AR-targeted therapies.

Acknowledgements

We thank Dr. H. Seimiya and Dr. S. Okabe (Cancer Chemotherapy Center, Japan) for kindly providing us with the PSA enhancer-promoter-Luc. This work was partly supported by a Grant-in-aid for Scientific Research on Innovative Areas "Chemical Biology of Natural Products" (Grant No. 23102006 to M.I.) from The Ministry of Education, Culture, Sports, Science and Technology, Japan.

Keywords: androgen receptor antagonists · cancer · drug resistance · natural products · NMR spectroscopy

How to cite: *Angew. Chem. Int. Ed.* **2016**, *55*, 2728–2732
Angew. Chem. **2016**, *128*, 2778–2782

[1] A. Jemal, R. Siegel, E. Ward, Y. Hao, J. Xu, T. Murray, M. L. Thun, *Ca-Cancer J. Clin.* **2008**, *58*, 71–96.
[2] C. A. Heinlein, C. Chang, *Endocr. Rev.* **2004**, *25*, 276–308.
[3] a) C. D. Chen, D. S. Welsbie, C. Tran, S. H. Baek, R. Chen, R. Vessella, M. G. Rosenfeld, C. L. Sawyers, *Nat. Med.* **2004**, *10*, 33–39; b) H. I. Scher, C. L. Sawyers, *J. Clin. Oncol.* **2005**, *23*, 8253–8261.
[4] M. E. Taplin, G. J. Bubley, Y. J. Ko, E. J. Small, M. Upton, B. Rajeshkumar, S. P. Balk, *Cancer Res.* **1999**, *59*, 2511–2515.
[5] a) M. Marcelli, M. Ittmann, S. Mariani, R. Sutherland, R. Nigam, L. Murthy, Y. Zhao, D. DiConcini, E. Puxeddu, A. Esen, J. Eastham, N. L. Weigel, D. J. Lamb, *Cancer Res.* **2000**, *60*, 944–949; b) Z. Culig, H. Klocker, G. Bartsch, A. Hobisch, *Am. J. Pharmacogenomics* **2001**, *1*, 241–249.
[6] C. Tran, S. Ouk, N. J. Clegg, P. A. Watson, V. Arora, J. Wongvipat, P. M. Smith-Jones, D. Yoo, A. Kwon, T. Wasielewska, D. Welsbie, C. D. Chen, C. S. Higano, T. M. Beer, D. T. Hung, H. I. Scher, M. E. Jung, C. L. Sawyers, *Science* **2009**, *324*, 787–790.
[7] T. Kawamura, T. Fujimaki, N. Hamanaka, K. Torii, H. Kobayashi, Y. Takahashi, M. Igarashi, N. Kinoshita, Y. Nishimura, E. Tashiro, M. Imoto, *J. Antibiot.* **2010**, *63*, 601–605.
[8] Y. Igarashi, L. Yu, M. Ikeda, T. Oikawa, S. Kitani, T. Nihira, B. Bayanmunkh, W. Panbangred, *J. Nat. Prod.* **2012**, *75*, 986–990.
[9] H. C. Kwon, C. A. Kauffman, P. R. Jensen, W. Fenical, *J. Am. Chem. Soc.* **2006**, *128*, 1622–1632.
[10] B. M. Trost, J. L. Belletire, S. Godleski, P. G. McDougal, J. M. Balkovec, J. J. Baldwin, M. E. Christy, G. S. Ponticello, S. L. Varga, J. P. Springer, *J. Org. Chem.* **1986**, *51*, 2370–2374.

[11] D. R. Scott, N. R. Bruce, I. R. Timothy, *Acc. Chem. Res.* **1998**, *31*, 9 – 17.
[12] L. Yu, M. E. Trujillo, S. Miyanaga, I. Saiki, Y. Igarashi, *J. Nat. Prod.* **2014**, *77*, 976 – 982.
[13] T. Yabuuchi, T. Kusumi, *J. Org. Chem.* **2000**, *65*, 397 – 404.
[14] N. Nagamine, T. Shirakawa, Y. Minato, K. Torii, H. Kobayashi, M. Imoto, Y. Sakakibara, *PLoS. Comput. Biol.* **2009**, *5*, e1000397.
[15] M. S. Ozers, B. D. Marks, K. Gowda, K. R. Kupcho, K. M. Ervin, T. D. Rosier, N. Qadir, H. C. Eliason, S. M. Riddle, M. S. Shekhani, *Biochemistry* **2007**, *46*, 683 – 695.
[16] T. Yoshida, H. Kinoshita, T. Segawa, E. Nakamura, T. Inoue, Y. Shimizu, T. Kamoto, O. Ogawa, *Cancer Res.* **2005**, *65*, 9611 – 9616.
[17] M. Korpal, J. M. Korn, X. Gao, D. P. Rakiec, D. A. Ruddy, S. Doshi, J. Yuan, S. G. Kovats, S. Kim, V. G. Cooke, J. E. Monahan, F. Stegmeier, T. M. Roberts, W. R. Sellers, W. Zhou, P. Zhu, *Cancer Discovery* **2013**, *3*, 1030 – 1043.

Received: October 29, 2015
Revised: November 19, 2015
Published online: January 25, 2016

